

Data-Driven Variable Impedance Control of a Powered Knee-Ankle Prosthesis for Sit, Stand, and Walk with Minimal Tuning

Cara G. Welker, T. Kevin Best, and Robert D. Gregg

Abstract—Although the average healthy adult transitions from sit to stand over 60 times per day, most research on powered prosthesis control has only focused on walking. In this paper, we present a data-driven controller that enables sitting, standing, and walking with minimal tuning. Our controller comprises two high level modes of sit/stand and walking, and we develop heuristic biomechanical rules to control transitions. We use a phase variable based on the user’s thigh angle to parameterize both walking and sit/stand motions, and use variable impedance control during ground contact and position control during swing. We extend previous work on data-driven optimization of continuous impedance parameter functions to design the sit/stand control mode using able-bodied data. Experiments with a powered knee-ankle prosthesis used by a participant with above-knee amputation demonstrate promise in clinical outcomes, as well as trade-offs between our minimal-tuning approach and accommodation of user preferences. Specifically, our controller enabled the participant to complete the sit/stand task 20% faster and reduced average asymmetry by half compared to his everyday passive prosthesis. The controller also facilitated a timed up and go test involving sitting, standing, walking, and turning, with only a mild (10%) decrease in speed compared to the everyday prosthesis. Our sit/stand/walk controller enables multiple activities of daily life with minimal tuning and mode switching.

I. INTRODUCTION

Over 600,000 Americans currently live with a major lower-limb amputation [1]. Because the passive and semi-active prostheses used by most people with amputation cannot supply net positive energy like biological joints, users compensate with their intact limb, leading to kinematic and kinetic asymmetries during walking [2], [3] and transitions between sitting and standing [4]–[6]. These compensatory behaviors can cause additional secondary complications like osteoarthritis and lower back pain [7]. Powered prostheses have the ability to supply net positive energy, and thus can reduce secondary complications and produce more normative movement [8]. However, the design of effective prosthetic control strategies, particularly for non-rhythmic tasks, remains a challenge. The majority of the research in this space has focused on control strategies for rhythmic locomotion [9], but almost half of movement bouts last less than 12 steps [10], and a healthy adult transitions from sit to stand

more than 60 times each day on average [11]. Therefore, in order to develop clinically viable prostheses, it is necessary to develop control strategies not only for rhythmic activities, but also for non-rhythmic ones such as sitting and standing.

Although sparse in the literature, there are examples of prior work investigating control strategies that allow an above-knee prosthesis user to transition between sitting and standing [12]–[15]. Most sit/stand control methods use a form of impedance control, which dictates the joint torque as a function of kinematic inputs of angular position θ and velocity $\dot{\theta}$, in addition to impedance parameters comprising stiffness K , damping B , and equilibrium angle θ_{eq} :

$$\tau = K(\theta_{eq} - \theta) - B\dot{\theta}. \quad (1)$$

Most sit/stand impedance controllers have separate control parameters for sit-to-stand and stand-to-sit, requiring real-time classification between the two modes [12], [13]. Varol et al. further subdivide each transition to sit or stand into multiple substates, an approach commonly used for walking controllers as well [16], [17]. Although tuning prosthesis parameters can be useful because individuals have distinct movement patterns, these prior approaches require significant tuning time, as three impedance parameters need to be tuned for each joint, substate, and activity [12], [16], [17]. Simon et al. use equilibrium angles corresponding with biological angles at the endpoints of the sit and stand motions and only tune stiffness and damping parameters, demonstrating that their controller reduces asymmetry during both sit-to-stand and stand-to-sit motions [13]. Varol et al. later extended their sit-to-stand framework to incorporate walking, which was able to correctly identify all transitions, but also detected an additional 7% of transitions that did not exist [18]. Hargrove et al. were able to reduce misclassification using surgical interventions along with an EMG classifier for additional activity modes [19].

Recently, Hunt et al. measured electromyography (EMG) from the intact biceps femoris as an input to a continuous controller that allowed users to transition between different activities such as sit, stand, walk, and lunge [14]. They demonstrated the efficacy of this controller to reduce muscle activation and improve loading symmetry during sit to stand in a single session. However, using electromyography as a real-time input signal has the limitations of drifting over time and needing frequent recalibration [20].

Aside from EMG control, another approach that allows for fewer distinct states and less switching is phase-based control. In this approach, the prosthetic joints are controlled by a phase variable that tracks the progression of the user’s

This work was supported by the National Institute of Child Health & Human Development of the NIH under Award Number R01HD094772 and by the National Science Foundation under Award Number 2024237. The content is solely the responsibility of the authors and does not necessarily represent the official views of the NIH and NSF.

Cara G. Welker, T. Kevin Best, and Robert D. Gregg are with the Department of Electrical Engineering and Computer Science and the Robotics Institute, University of Michigan, Ann Arbor, MI 48109. Contact: {cgwelker, tkbest, rdgregg}@umich.edu

motion. Because the phase variable is a biological signal controlled by the user, this allows for some amount of volitional control not only for rhythmic tasks, but also for non-rhythmic start and stop motions [21] and gait perturbations [22]. Previous work has shown thigh angle to be an appropriate phase variable to control lower-limb powered prostheses during gait [21], [23]–[27]. Thigh angle has also been proposed as a phase variable in a position controller for sit/stand [15], but this controller was not experimentally validated. The sit/stand controller in [13] used axial load as a form of phase variable, but it is unclear if this would be an appropriate choice for walking, and only sit/stand was tested.

In this manuscript, we present a continuous control framework for a powered knee-ankle prosthesis that enables sitting, standing, and walking, as well as transitions between them. We integrate two control modes – a previously developed walking mode [25], and a novel mode for sitting and standing motions. This integrated controller enables investigation of additional clinical metrics such as the timed up and go (TUG) test. This test has been shown to correlate with fall risk in multiple populations, including those with amputation [28], [29], but is rarely tested with powered prostheses because different control modes are not integrated.

This paper’s contributions include: 1) An integrated knee-ankle prosthesis controller that enables sitting, standing, and walking with autonomous transitions. 2) A novel, unified sit/stand control mode that extends a control framework used in walking based on data-driven impedance control and phase variable parameterization. 3) Experimental validation of the sit/stand mode with an above-knee prosthesis user enabling faster movement and reduced overall asymmetry compared to a passive prosthesis, and kinematics and kinetics with similar trends to able-bodied motion. 4) Demonstration of the combined controller to enable an above-knee prosthesis user to perform a clinical TUG test, with only modest reductions in speed compared to a passive prosthesis.

II. SIT/STAND/WALK CONTROLLER

We present a continuous controller capable of both walking and sit/stand movements, driven by a phase variable based on the user’s thigh angle. Our controller, consisting of a walking and a sit/stand mode, uses a high-level FSM to select between modes based on biomechanical cues. Our novel sit/stand mode uses variable impedance control, while the walking mode uses variable impedance control during stance and position control during swing [25]. Both controllers utilize able-bodied datasets in their construction with the aim of replicating normative motions and reducing compensations associated with passive prosthesis use [2]–[6]. Together, the walking and sit/stand mode allow the prosthesis to autonomously transition between walking, sitting, and standing, thus enabling an array of activities of daily living.

In this work, we focus on the high-level control logic that selects between walking and sit/stand modes, as well as the novel sit/stand mid-level control architecture. For brevity, we omit details of the walking mode control logic, but refer the interested reader to [25] for a thorough explanation. During

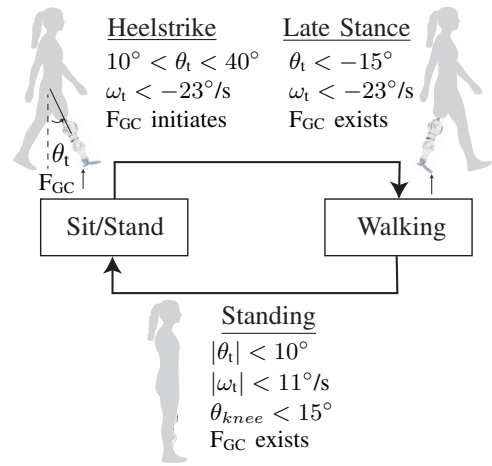


Fig. 1. A diagram of the high-level control FSM that dictates transitions between walking and sit/stand modes, determined by the thigh angle θ_t and angular velocity ω_t , knee angle θ_k , and foot ground contact (F_{GC}). We use these signals to detect prosthetic-side heelstrike or late stance to transition to walking. We transition to standing when the user is stationary with prosthesis ground contact, a vertical thigh, and an extended knee.

mode transitions, we calculate output torque as a weighted sum of each mode’s output torque that linearly varies over 200 ms to produce a smooth torque transition.

A. High-level Mode Selection

To select between the sit/stand and walking modes, we use a high-level FSM with two modes to determine the user’s intent based on prosthesis sensor readings (Fig. 1). By limiting the FSM to two control modes, we reduce complexity and the chances of the controller making an incorrect transition decision, which could produce undesirable or dangerous behavior. We developed transition rules based on input signals available from the powered knee-ankle prosthesis later used in experimental testing [30]. These signals include the global thigh angle θ_t and angular velocity ω_t obtained from an inertial measurement unit (IMU) at the proximal end of the knee joint, the knee angle θ_k measured from the joint encoder, and foot contact F_{GC} determined by the load cell at the distal end of the ankle joint. The threshold used for making F_{GC} was 75 N, while the threshold for breaking F_{GC} was 25 N. Using these input signals, we heuristically determined transition criteria with previously collected data of amputee gait, as well as pilot testing with an able-bodied participant using a bypass adaptor, which mounts the prosthesis under an intact knee in a flexed position.

We include two stand to walk transition criteria, as the user can initiate movement by leading with either the prosthetic or biological leg (Fig. 1). Thus, the FSM transitions from the sit/stand mode to the walk mode if either prosthetic-side heel strike (HS) or late stance is detected. We define a heelstrike transition to walking by a rising edge in the foot contact signal F_{GC} while $10 < \theta_t < 40$ deg (flexion) and $\omega_t < -23$ deg/sec (extension). The upper bound on thigh angle prevents erroneous transitions to walk mode while the user is seated. We define prosthetic-side late stance transition to walking if $\theta_t < -15$ deg and $\omega_t < -23$ deg/sec (extension).

We use only one set of criteria to detect a transition from walking to the sit/stand mode. Specifically, the FSM transitions when $|\theta_t| < 10$ deg, $|\omega_t| < 11$ deg/sec, and the foot is in contact with the ground, conditions indicative of upright stance. To prevent rapid state machine switching that could occur if the user paused during toe-off, we also do not allow a transition to the sit/stand mode if $\theta_k > 15$ deg.

B. Sit/Stand Control Mode

We sought to develop a continuous, variable impedance sit/stand controller by creating a data-driven impedance model with a phase variable as input, and continuous impedance parameters as outputs. In contrast with prior work, which either treats sit-to-stand and stand-to-sit as separate controllers that need to be individually tuned [13], [16] or require EMG input [14], our unified sit/stand mode uses thigh angle as a phase variable and impedance control derived from able-bodied data. First, we extend the concept of gait phase to sitting and standing motions. Then, we process a previously collected dataset of able-bodied sitting and standing kinematics and kinetics, which we use in an optimization to calculate stiffness, damping, and equilibrium angle functions for the knee and ankle. Evaluating these functions at a given phase estimate allows us to calculate joint torque using the impedance control equation (1).

1) *Phase Variable*: As in the previously developed walking mode [25], we use a phase variable based on the user’s prosthetic global thigh angle θ_t to parameterize the controller’s behavior during sit/stand motions. The global thigh angle is an appropriate choice for a phase variable, as it monotonically increases during sit-to-stand motions and monotonically decreases during stand-to-sit motions. During sit/stand, s represents the user’s location between a sitting state ($s = 0$) and a standing state ($s = 1$). The phase variable can increase or decrease, making both sit-to-stand and stand-to-sit motions possible with one controller. Similar to previous work in walking controllers [21], [24], [25], we define s through an affine transformation of θ_t :

$$s = (\theta_t^0 - \theta_t)/(\theta_t^0), \quad (2)$$

where θ_t^0 is the user’s thigh angle when sitting comfortably in a chair. Due to the closed chain kinematics of sitting, this angle depends on both the user’s leg dimensions and the chair height. Currently, θ_t^0 is measured by a researcher during a seated position, but future work could automate this update to account for different user sizes and chair dimensions.

2) *Able-Bodied Dataset Processing*: To create a sit/stand impedance model, we adapt a previously collected dataset of kinematics and kinetics from ten able-bodied participants transitioning from sit to stand and stand to sit 5 times each at a self-selected pace [31]. From these data, we use sagittal plane kinematics and kinetics for the knee and ankle joints, and calculate global thigh angle in the sagittal plane using the hip and torso kinematic data. We normalize joint torques by subject mass and differentiate and filter joint angles with a fourth order Butterworth low-pass filter to obtain angular velocities. As 5-6 Hz is frequently used as a cutoff frequency

during walking [32], we choose a cutoff frequency of 2 Hz due to the slower frequency content of sit and stand transitions.

Next, we segment these data to determine the start and end of the sit-to-stand and stand-to-sit motions. Previous work with this dataset used hip and knee angles to determine the start and end of the sit-to-stand motion [31], but we instead use signals derived from our phase variable (i.e., normalized global thigh angle) to segment the data. The start and end of the motion was defined when the thigh angular velocity crossed a threshold of 5 deg/sec before and after each motion, respectively. In addition, as some subjects consistently reported a knee flexion angle much larger than zero during standing, we subtracted out each subject’s average minimum knee angle over all five trials. The final dataset contained 100 trials, half sit-to-stand motions and half stand-to-sit motions.

3) *Impedance Model Optimization*: Similar to [25], we model the impedance parameters (K , B , and θ_{eq}) as continuous fourth order polynomials of phase s , where each polynomial is defined through a set of constant coefficients $\kappa = \{k_i, b_i, e_i | 0 \leq i \leq 4\}$:

$$K(s) = \sum_{i=0}^4 k_i s^i, \quad B(s) = \sum_{i=0}^4 b_i s^i, \quad \theta_{eq}(s) = \sum_{i=0}^4 e_i s^i. \quad (3)$$

To select the coefficients, we construct a data-driven optimization problem using all 100 trials of sitting and standing data. This optimization problem selects κ such that the impedance control equation (1) best reproduces the normalized torque profiles τ given the joint angles θ and angular velocities $\dot{\theta}$ for each trial in the dataset:

$$\kappa^* = \arg \min \|\tau - \hat{\tau}\|_2^2, \quad (4)$$

where $\hat{\tau} = K(s)(\theta_{eq}(s) - \theta) - B(s)\dot{\theta}$.

Instead of assuming that s progresses linearly in time as in [24], [25], here we calculate s using the dataset thigh kinematics with (2) to allow the optimization to internally account for thigh trajectory nonlinearities. A detailed discussion of how we efficiently solve this optimization problem through a change of variables to induce convexity is presented in [25] and is omitted here for brevity. Although (4) may have many “good” local minima, the convex approximation ensures a globally optimal solution. We calculate the solution three times, once with the sit-to-stand data, once with the stand-to-sit data, and once including both sets of data, to investigate the feasibility of using a unified model for both directions.

We add constraints to the optimization problem based on desired controller behavior and pilot testing with the bypass adaptor to ensure reasonable impedance trajectories for the given task. Namely, we constrain stiffness to be greater than 0.0087 Nm/(deg·kg) at the knee and 0.0175 Nm/(deg·kg) at the ankle. We constrain damping to be between $1.75 \cdot 10^{-4}$ and $2.6 \cdot 10^{-3}$ Nm·sec/(deg·kg) for both joints. Finally, we add constraints to ensure that (1) produces no torque at either joint when $s = 0$ (sitting) and no torque at the knee when $s = 1$ (standing). Given the non-zero stiffness and damping

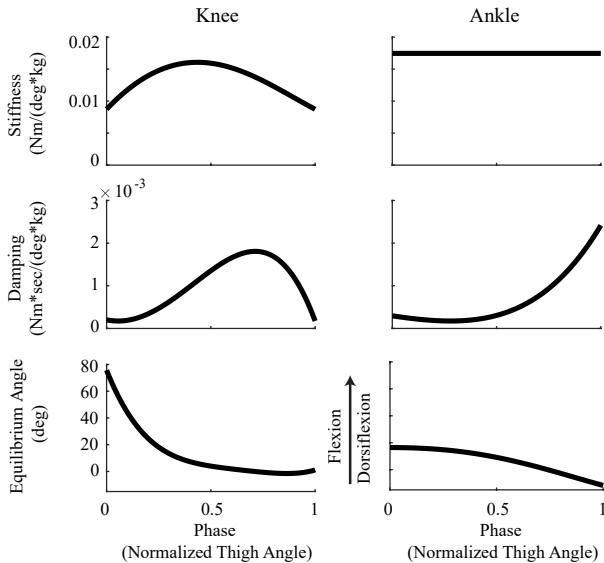


Fig. 2. Final optimal trajectories for stiffness, damping, and equilibrium angle for the knee and ankle joint are plotted during the sit-to-stand motion with respect to the phase variable of normalized thigh angle. Positive equilibrium angles correspond to knee flexion and ankle dorsiflexion. Phase is 0 while sitting and 1 while standing.

constraints, these constraints indirectly constrain $\theta_{eq}(0)$ for both joints and $\theta_{eq}(1)$ for the knee to be equal to the mean sitting and standing joint angles, respectively.

Fig. 2 shows the calculated optimal impedance parameters functions for both joints based on the combined sitting and standing data. Although most parameters vary significantly with phase, it is interesting to note that the optimal ankle stiffness maintains a static value at the minimum constraint. We hypothesize that this is due to the fact that the ankle torque in the dataset was fairly small in magnitude and inconsistent in direction. While this suggests that lowering the minimum stiffness could have increased our fit to the dataset, a controller with very low stiffness would be unable to reject disturbances or robustly handle inter-subject variation.

To determine goodness of fit of our optimization results, we calculated the model joint torque using (1), (3), and κ^* at each point in the dataset. We compared the root mean squared error (RMSE) of our model torque to typical human variation by normalizing it by the standard deviation of the joint torque seen in the dataset. The resulting normalized RMSE was 1.26 for the ankle and 1.67 for the knee when optimizing using the sit-to-stand data, and 1.46 for the ankle and 1.18 for the knee when optimizing using the stand-to-sit data. The normalized RMSE for the optimization using the combined data was similar (1.34 for the ankle and 1.39 for the knee). Because the combined solution with one set of parameters simplifies the controller state machine with only a small tradeoff in model fit, we use the combined model for the subsequent experiment.

III. EXPERIMENTAL PROTOCOL

To demonstrate proof-of-concept, we implemented our controller on a previously developed powered knee-ankle

prosthesis that has been validated for open-loop impedance control [30]. We conducted an experiment with one 26-year-old male participant with a left-side above-knee amputation, who was 1.9 meters tall with a mass of 113 kg while wearing his standard prosthesis (an Ottobock C-Leg 4 with an Ottobock Trias foot). His cause of amputation was congenital, and he had a clinical score of K4 on Medicare’s 5-point scale, corresponding with the highest mobility function. The experimental protocol was approved by the Institutional Review Board of the University of Michigan (HUM00166976), and the participant wore a ceiling-mounted safety harness for the duration of the experiment. A certified prosthetist assisted in fitting the powered prosthesis and ensured the safety of the participant throughout the experiment.

The experimental protocol investigated sit-to-stand, stand-to-sit, walking, and turning motions while the participant wore either his standard prosthesis or the powered prosthetic leg. Specifically, we investigated whether our controller could elicit motions similar to able-bodied, and how it compared to the participant’s standard prosthesis in functional metrics. Because passive and semi-active above-knee prostheses are associated with increased asymmetry and completion time in sit/stand transitions compared to able-bodied movement [4]–[6], we investigated both of these metrics. In addition, we conducted TUG tests with both prostheses, as this is a common clinical metric that combines sitting, standing, walking, and turning motions and is correlated with fall risk [28], [29].

The protocol took place over one two-hour session. During the sit/stand data collection, we used an armless chair adjusted to a height approximately equal to the participant’s knee height to match our model input data [31] (Fig. 3). After donning and aligning the powered prosthetic leg with the help of the prosthetist, the participant acclimated to the sit/stand behavior of the controller. During this acclimation period, the participant noted that while the assistive torque provided by the controller in the sit-to-stand motion felt helpful, the equivalent resistive torque slowing the stand-to-sit motion made it difficult to complete the task. In order to allow the participant to sit, the model mass of the participant was reduced by 40% to reduce the output torques.

After acclimation, the participant spent 10 minutes training to maximize the loading symmetry of his sit/stand motions using visual feedback. Specifically, he was asked to keep one foot on each of two ground-embedded force plates (AMTI, MA, USA) from which 3-axis force and moment data were collected at 250 Hz. The participant was able to see his level of loading symmetry calculated from these force plate data as a sliding bar on a screen in front of him (see Fig. 3). During perfectly symmetrical loading on both feet, the bar was centered on the screen and turned green. If one foot was loaded significantly more than the other, the bar’s position moved in the direction of higher loading and gradually transitioned from green to red with increasing asymmetry.

After training, the participant took a brief break and the visual feedback was removed. The participant was instructed to keep one foot on each force plate and evenly load both

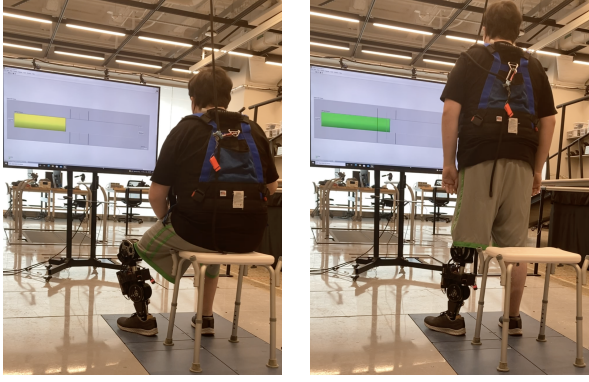


Fig. 3. Photos of the participant practicing sit/stand symmetry with the powered prosthesis during training. The bar on the screen depicted the real-time loading symmetry between the left and right foot. When the loading symmetry was outside the recommended range ($\pm 15\%$), the bar turned yellow and then gradually red as it moved away from the centerpoint.

legs during the sitting and standing motions as much as possible in the absence of feedback. Testing consisted of five repetitions of the sit-to-stand and stand-to-sit motions in two different conditions, with a break in between. In the first condition, termed the relaxed condition, the sitting and standing motions were performed discretely, as the experimenter provided cues to initiate each motion three seconds after the participant fully reached a sitting or standing position. In the second condition, termed the rapid condition, we conducted a clinical 5 times sit-to-stand test (5xSS), asking the participant to sit and stand five times as fast as comfortably possible with his hands crossed over his chest.

The second part of the protocol involved a combination of sitting, standing, walking, and turning tasks in a TUG test. During an acclimation period, the participant was informed of the high-level transition behavior of the controller and practiced initiating walking with both legs, as well as stopping and turning. All of these motions were combined in the TUG test, in which the participant started from a seated position, stood up, walked 6 meters to a line on the floor, turned around, walked back, and sat down. Verbal instructions were based on CDC guidelines for this clinical test and instructed the participant to “walk at a comfortable pace.” After practice, the participant completed five TUG tests with a brief break in between each. An experimenter timed these tests from the verbal cue to start until the participant returned to a fully seated position.

After completing the above protocol with the powered prosthesis, the participant repeated the procedure using his standard prosthesis. An equal amount of symmetry training time was given, but the sit/stand and transition acclimation periods were eliminated, as the participant was already accustomed to his standard prosthesis due to daily use.

IV. EXPERIMENTAL RESULTS

A. Powered Prosthesis Similarity to Able-Bodied Mechanics

We segmented the sit/stand data from the relaxed condition trials into discrete sitting and standing motions in the same

manner as the able-bodied dataset (discussed in Section II-B.2). The powered prosthetic leg recorded the commanded torques and measured joint angles for the ankle and knee. We then compared the resulting phase estimate and average kinematics and kinetics during the sit-to-stand and stand-to-sit motions to the able-bodied dataset (Fig. 4). As the knee performs more work than the ankle during sit/stand [31], we also calculated net knee joint work during both motions, finding that the powered prosthesis provided a similar magnitude of negative joint work during stand-to-sit (0.47 ± 0.05 J/kg) compared to the able-bodied dataset (0.49 ± 0.19 J/kg) and $\sim 60\%$ of the positive joint work during sit-to-stand (0.31 ± 0.06 J/kg compared to 0.54 ± 0.17 J/kg).

The phase variable observed during the experiment is similar to the expected phase trajectory calculated from able-bodied data, which is important in producing the correct impedance parameters from the model. However, the experimental phase variable never fully reached 1 during standing, and slight periods of saturation exist near $s = 0$. The knee kinematics match the able-bodied dataset relatively well, and the knee kinetics demonstrate similar trends. However, we see a slight delay in the assistive knee torque during sit-to-stand, and reduced overall magnitude of knee torque during both motions due to the reduced model mass used to achieve stand-to-sit. Ankle kinematics and kinetics during $s = 0$ suggest that the participant was standing with a more posterior center of pressure than the able-bodied comparisons, causing reduced ankle dorsiflexion in the kinematics and reduced ankle plantarflexion torque.

B. Functional Comparisons Between Prostheses

Additionally, we compared functional outcome metrics, such as leg loading symmetry and task completion time, between the trials performed with the powered prosthesis and with the participant’s standard passive prosthesis. Because kinematic data were not available from the passive prosthesis, we segmented the sit/stand motions in these trials using the collected force plate data in the vertical direction. These three force plates were positioned under the chair ($F_{z,\text{chair}}$), the biological limb ($F_{z,\text{bio}}$), and the prosthetic limb ($F_{z,\text{prosth}}$).

Because the rapid sit-to-stand test was conducted as one continuous motion, we segmented the data into sit-stand-sit cycles. We defined the start and end of the continuous motion when $F_{z,\text{chair}}$ leaves or enters steady state, respectively (defined when the derivative of $|F_{z,\text{chair}}| < 50$ N/s). The remaining data were then segmented by finding the midpoint of the sections where $F_{z,\text{chair}}$ was nonzero. Using this segmentation method, we determined that the time to complete one full cycle of sit-stand-sit in the 5xSS test was reduced by 20% with the powered prosthesis (4.0 ± 0.2 sec) compared to the passive prosthesis (5.0 ± 0.5 sec).

For the relaxed trials, the start of sit-to-stand was determined when $F_{z,\text{chair}}$ decreased while both $F_{z,\text{bio}}$ and $F_{z,\text{prosth}}$ increased. The end of stand-to-sit was determined when the chair force entered steady state (as defined above). Steady-state standing was determined when the time derivative of the

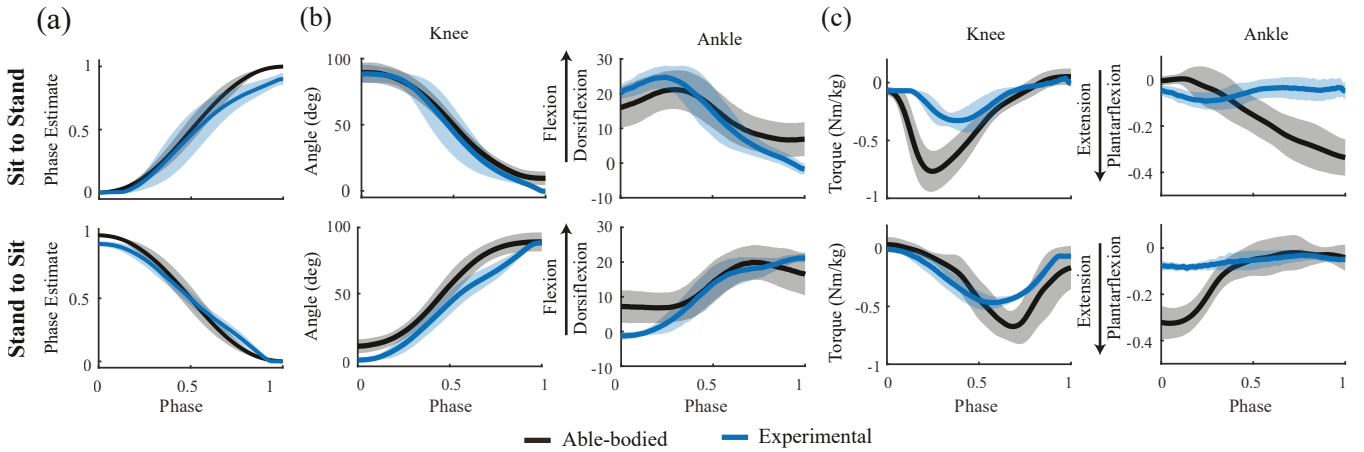


Fig. 4. Comparisons between the behavior of our controller implemented on the powered prosthesis during relaxed sit/stand motions to the mean able-bodied data used in the impedance model development [31]. (a) Trajectory of the phase estimate, determined by normalized thigh angle. (b) Kinematic data at the knee and ankle joint. (c) Kinetic data at the knee and ankle joint. Shaded regions represent ± 1 standard deviation.

summed forces of both legs stabilized ($|F_{z,\text{prosth}} + F_{z,\text{bio}}| < 300$ N/s). The ground reaction forces during the duration of sit-to-stand and stand-to-sit for each leg are shown in Fig. 5. We note that the steady-state standing detection was very sensitive to the threshold used, and prior work using this segmentation method does not specify the threshold [13]. However, with our chosen threshold, the time required for both sit-to-stand and stand-to-sit was similar between the passive and powered conditions during the relaxed trials.

For each relaxed trial, we calculated the degree of leg loading asymmetry (DoA), defined as

$$DoA = (F_{z,\text{bio}} - F_{z,\text{prosth}}) / (F_{z,\text{bio}} + F_{z,\text{prosth}}). \quad (5)$$

A positive DoA value corresponds to increased loading of the biological limb and a negative value corresponds with increased loading of the prosthetic limb, while $DoA = 0$ indicates perfectly balanced loading of both limbs. For both sit-to-stand and stand-to-sit, we report average asymmetry, as well as RMS loading of the prosthetic leg over the motion as in [14].

RMS loading of the prosthetic leg increased with the powered versus passive prosthesis during both relaxed sit-to-stand ($35.0 \pm 5.3\%$ versus $27.4 \pm 3.1\%$ bodyweight) and stand-to-sit ($34.2 \pm 1.3\%$ versus $28.0 \pm 3.0\%$ bodyweight). Average asymmetry with the powered prosthesis was also reduced compared to the passive prosthesis for relaxed sit-to-stand (0.43 ± 0.06 versus 0.27 ± 0.11) and stand-to-sit (0.40 ± 0.06 versus 0.22 ± 0.03). Even when the participant was primarily focused on speed in the rapid condition, similar magnitudes of average asymmetry reduction were seen for the duration of the sit-stand-sit motion (0.38 ± 0.02 versus 0.18 ± 0.05).

Finally, the mean TUG time achieved with the powered prosthesis was slightly slower than with the passive prosthesis (21.4 ± 0.4 sec with powered, 19.3 ± 0.5 sec with passive). The supplementary video shows that much of this time discrepancy occurred during the standing and turning portions of the test, which suggests that the differences may

be due more to balance and trust with the powered prosthesis than the controller behavior. We also note that the high-level FSM made no misclassifications during the TUG test.

V. DISCUSSION

Amputee experiments with the proposed controller demonstrate that our novel sit/stand mode enables faster motions and reduced overall asymmetry compared to a passive prosthesis. The participant was also able to transition between walking, sitting, and standing with our controller. Our approach is unique from prior works on sit/stand controllers for powered knee-ankle prostheses, which typically require separate state detection and manually tuning parameters for sit-to-stand and stand-to-sit [13], [16]. Instead, we combine sitting and standing in a unified control mode using a thigh angle phase variable that can progress forward or backward. We justify this decision in the impedance parameter optimization from able-bodied data, which showed only a small trade-off in RMSE compared to separately designed control modes. We believe this trade-off is justified for decreased controller complexity, which could reduce errors caused by incorrect switching between sitting and standing states, and note that our controller always correctly identified sit/stand versus walk mode during the TUG tests.

However, the amputee experiment revealed shortcomings of the unified sit/stand approach that were not observed during pilot testing with able-bodied participants in a bypass adapter. Theoretically, the controller has no tunable parameters; it requires only an input user mass as a multiplier to the normalized joint torques and a measured baseline thigh angle while sitting to define the phase variable. In the able-bodied pilot trials, these input measurements allowed the controller to produce normative positive work during sit-to-stand and negative work during stand-to-sit. However, the participant with amputation noted that, while the assistance felt appropriate during sit-to-stand, the controller impeded his ability to transition from stand to sit. Therefore, we reduced the input mass to the impedance sit/stand model by 40%, allowing him

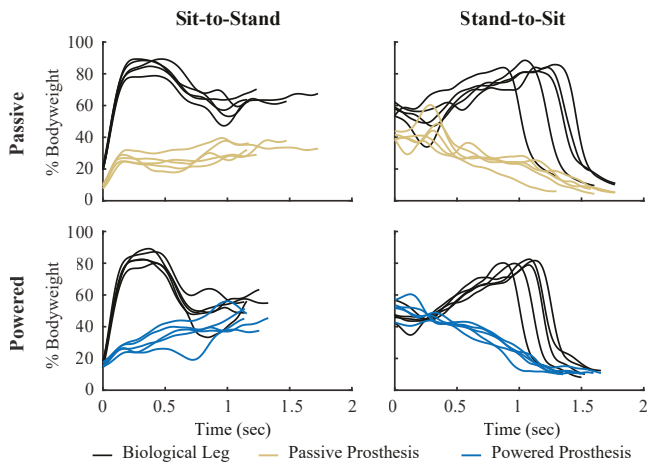


Fig. 5. Vertical loading for the biological and prosthetic leg over time is shown for the relaxed condition of both sit-to-stand and stand-to-sit. Although peak loading asymmetry is similar between the passive and powered prostheses, the powered prosthesis enables the user to reach symmetry more quickly for both sit-to-stand and stand-to-sit.

to complete the stand-to-sit motion. This reduction resulted in overall lower applied torques compared to prior sit/stand controllers, although these controllers demonstrate a large variation in maximum torque at the knee between less than 0.4 Nm/kg [12] to almost 1 Nm/kg [13], [14].

Although our overall joint torques were lower due to the reduction in model mass, our controller still commanded larger torques at the knee compared to able-bodied at the beginning of stand-to-sit (Fig. 4), which would have impeded the participant’s ability to sit down without reducing the modeled mass. Because of this, our controller produced similar mechanical work to able-bodied comparisons in stand-to-sit even with the reduced mass. We hypothesize that this is due to an underestimation in phase at the beginning of the motion, due to the subject’s thigh angle never reaching one (Fig. 4(a)). The experimental ankle kinematics and kinetics during standing also support this hypothesis and demonstrate that the center of pressure of the participant was more posterior compared to able-bodied data. Although we conducted symmetry training of the loading between the left and right foot, we gave the participant no instructions on anterior/posterior center of pressure placement. This discrepancy could possibly be mitigated by additional training or adapting the phase variable normalization based on the standing thigh angle.

Despite these discrepancies in the controller behavior relative to able-bodied comparisons, the functional tests demonstrated an improvement in timing and overall asymmetry compared to the participant’s passive prosthesis. Prior work demonstrated a reduction in asymmetry at peak vertical acceleration [13], which remains largely unchanged with our powered controller (Fig. 5). However, the powered prosthetic leg loading of 35% bodyweight seen with our controller during sit-to-stand was similar to previous work that demonstrated loading between 30-35% [14]. In addition, this is the first demonstration of a sit/stand prosthesis controller with

improvements in timing, which is a predictor of balance [33]. The ground reaction forces over the duration of the sit-to-stand motion demonstrate that the powered prosthesis enabled the participant to reach loading symmetry more quickly at the end of the sit-to-stand motion (Fig. 5). We hypothesize that this loading symmetry allowed him to reach a stable position from sit-to-stand more quickly to then begin the stand-to-sit movement, which may have contributed to improvements in timing in the rapid sit-to-stand test.

A limitation of the sit/stand testing was that only one chair height was examined, and we manually zeroed the phase variable while the participant was comfortably seated. In future work, this process could be automated so that the phase variable automatically adapts while the user is seated, and could treat chair height as a task variable similar to previous work on changing speeds and inclines in walking [24], [25]. Although the prosthesis would not be switching modes between sit and stand, a seated resting position would need to be detected in order to accomplish this automated update. In addition, we demonstrated improved functional outcomes with a minimal tuning approach, but additional individualization capabilities could yield improved outcomes. Future work should investigate if it is possible to individualize the impedance trajectories in a time-efficient manner.

The focus of this work was the novel sit/stand control mode, but we also demonstrated a proof of concept for using our continuous controller to complete a TUG test consisting of sitting, standing, walking, and turning (Fig. 1). While our controller resulted in a 2.1 second increase in time to complete this test, the supplemental video data shows that much of this additional time was spent turning, which was not modeled and only minimally experimentally trained. TUG times with both the passive and powered prosthesis were above the 19-second threshold associated with greater fall risk for amputees [29]. In addition, the powered knee-ankle prosthesis only has sagittal plane degrees of freedom; if the user is turning and the direction of power provided is not aligned with the heading direction, this may create instability in the mediolateral direction. Incorporating additional degrees of freedom, training time, or modeling of turning behavior in future work could increase performance.

Another limitation is that we only tested one participant with amputation, so the controller behavior and clinical outcomes may not generalize to the wider population. In particular, this participant’s mass was higher than average for the general population and our input dataset, which resulted in higher magnitude impedance parameters since torque is normalized by participant mass. In addition, this participant is classified as a K4 on the community ambulation scale, corresponding with the highest degree of mobility. Finally, although we provided a brief period of acclimation and training, results may improve with additional training, which should be the focus of future work.

VI. CONCLUSION

In this work, we developed a continuous controller for a powered knee-ankle prosthesis that enables both sit/stand

and walking activities through continuous, phase-based impedance and kinematic control. This controller is unique from prior work in that it contains only two high level modes consisting of sit/stand and walking, and requires minimal manual tuning of controller parameters. We developed heuristic rules based on biomechanical cues to transition between modes and calculated optimal impedance parameter trajectories based on able-bodied data. We conducted experiments with one individual with an amputation, demonstrating faster and overall more symmetric transitions between sit and stand, with increased prosthesis loading. However, our experimental results indicate that the advantages of our limited tuning approach with combined sit/stand states come at the cost of limited ability to accommodate user preferences that differ from the input dataset. Finally, we demonstrated that the continuous controller allowed the participant to perform a TUG test, which involved sit-to-stand, stand-to-sit, walking, and turning motions.

ACKNOWLEDGEMENT

The authors thank Friedl De Groot for providing the identified sit/stand data for the model development, Leslie Wontorcik, CP, for clinical support during experiments, and our participant for making this experiment possible.

REFERENCES

- [1] K. Ziegler-Graham, E. J. MacKenzie, P. L. Ephraim, T. G. Trivison, and R. Brookmeyer, "Estimating the Prevalence of Limb Loss in the United States: 2005 to 2050," *Arch. Phys. Med. Rehabil.*, vol. 89, no. 3, pp. 422–429, 2008.
- [2] M. Schaarschmidt, S. W. Lipfert, C. Meier-Gratz, H. C. Scholle, and A. Seyfarth, "Functional gait asymmetry of unilateral transfemoral amputees," *Hum. Movement Sci.*, vol. 31, no. 4, pp. 907–17, 2012.
- [3] K. R. Kaufman, S. Frittoli, and C. A. Frigo, "Gait asymmetry of transfemoral amputees using mechanical and microprocessor-controlled prosthetic knees," *Clin. Biomech.*, vol. 27, no. 5, pp. 460–5, 2012.
- [4] H. Burger, J. Kuželický, and Č. R. Marinek, "Transition from sitting to standing after trans-femoral amputation," *Prosthet. Orthot. Int.*, vol. 29, no. 2, pp. 139–51, 2005.
- [5] M. Highsmith *et al.*, "Kinetic asymmetry in transfemoral amputees while performing sit to stand and stand to sit movements," *Gait Posture*, vol. 34, no. 1, pp. 86–91, 2011.
- [6] E. J. Wolf, V. Q. Everding, A. A. Linberg, J. M. Czerniecki, and C. J. M. Gambel, "Comparison of the Power Knee and C-Leg during step-up and sit-to-stand tasks," *Gait Posture*, vol. 38, no. 3, pp. 397–402, 2013.
- [7] R. Gailey, K. Allen, J. Castles, J. Kucharik, and M. Roeder, "Review of secondary physical conditions associated with lower-limb amputation and long-term prosthesis use," *J. Rehabil. Res. Dev.*, vol. 45, no. 1, pp. 15–29, 2007.
- [8] R. R. Torrealba and E. D. Fonseca-Rojas, "Toward the Development of Knee Prostheses: Review of Current Active Devices," *Appl. Mech. Rev.*, vol. 71, no. 3, pp. 1–22, 2019.
- [9] M. Tucker *et al.*, "Control strategies for active lower extremity prosthetics and orthotics: A review," *J. Neuroeng. Rehabil.*, vol. 12, no. 1, 2015.
- [10] M. S. Orendurff, J. A. Schoen, G. C. Bernatz, A. D. Segal, and G. K. Klute, "How humans walk: Bout duration, steps per bout, and rest duration," *J. Rehabil. Res. Dev.*, vol. 45, no. 7, pp. 1077–1090, 2008.
- [11] P. M. Dall and A. Kerr, "Frequency of the sit to stand task: An observational study of free-living adults," *Appl. Ergon.*, vol. 41, no. 1, pp. 58–61, 2010.
- [12] H. A. Varol, F. Sup, and M. Goldfarb, "Powered sit-to-stand and assistive stand-to-sit framework for a powered transfemoral prosthesis," in *Int. Conf. Rehab. Robot.*, 2009, pp. 645–651.
- [13] A. M. Simon, N. P. Fey, K. A. Ingraham, S. B. Finucane, E. G. Halsne, and L. J. Hargrove, "Improved Weight-Bearing Symmetry for Transfemoral Amputees during Standing Up and Sitting Down with a Powered Knee-Ankle Prosthesis," *Arch. Phys. Med. Rehabil.*, vol. 97, no. 7, pp. 1100–6, 2016.
- [14] G. Hunt, S. Hood, and T. Lenzi, "Stand-up, squat, lunge, and walk with a robotic knee and ankle prosthesis under shared neural control," *IEEE Open J. Eng. Med. Biol.*, vol. 2, pp. 267–277, 2021.
- [15] D. Raz, E. Bolívar-Nieto, N. Ozay, and R. D. Gregg, "Toward phase-variable control of sit-to-stand motion with a powered knee-ankle prosthesis," in *IEEE Conf. Control Technol. Appl.*, 2021, pp. 627–633.
- [16] F. Sup, H. Varol, J. Mitchell, T. Withrow, and M. Goldfarb, "Self-contained powered knee and ankle prosthesis: Initial evaluation on a transfemoral amputee," *IEEE Int. Conf. Rehabil. Robot.*, pp. 638–644, 2009.
- [17] A. Simon *et al.*, "Configuring a powered knee and ankle prosthesis for transfemoral amputees within five specific ambulation modes," *PLoS One*, vol. 9, no. 6, 2014.
- [18] H. A. Varol, F. Sup, and M. Goldfarb, "Multiclass real-time intent recognition of a powered lower limb prosthesis," *IEEE Transactions on Biomedical Engineering*, vol. 57, no. 3, pp. 542–551, 2010.
- [19] L. J. Hargrove *et al.*, "Robotic Leg Control with EMG Decoding in an Amputee with Nerve Transfers," *New England Journal of Medicine*, vol. 369, pp. 1237–1242, 2013.
- [20] J. A. Spanias, E. J. Perreault, and L. J. Hargrove, "Detection of and Compensation for EMG Disturbances for Powered Lower Limb Prosthesis Control," *IEEE T. Neural Syst. Rehabil. Eng.*, vol. 24, no. 2, pp. 226–234, 2016.
- [21] S. Rezaazadeh, D. Quintero, N. Divekar, E. Reznick, L. Gray, and R. D. Gregg, "A phase variable approach for improved rhythmic and non-rhythmic control of a powered knee-ankle prosthesis," *IEEE Access*, vol. 7, pp. 109 840–109 855, 2019.
- [22] D. J. Villarreal, H. A. Poonawala, and R. D. Gregg, "A Robust Parameterization of Human Gait Patterns Across Phase-Shifting Perturbations," *IEEE Trans. Neural Syst. Rehabil. Eng.*, vol. 25, no. 3, pp. 265–278, 2017.
- [23] D. Quintero, D. J. Villarreal, D. J. Lambert, S. Kapp, and R. D. Gregg, "Continuous-Phase Control of a Powered Knee-Ankle Prosthesis: Amputee Experiments Across Speeds and Inclines," *IEEE Trans. Robot.*, vol. 34, no. 3, pp. 686–701, 2018.
- [24] T. Best, K. Embry, E. Rouse, and R. Gregg, "Phase-variable control of a powered knee-ankle prosthesis over continuously varying speeds and inclines," *IEEE Int. Conf. Intell. Robot. Sys.*, 2021.
- [25] T. Best, C. Welker, E. Rouse, and R. Gregg, "Phase-based impedance control of a powered knee-ankle prosthesis for tuning-free locomotion over speeds and inclines," 2022. [Online]. Available: <https://doi.org/10.36227/techrxiv.19165895.v1>
- [26] W. Hong, N. Anil Kumar, and P. Hur, "A Phase-Shifting Based Human Gait Phase Estimation for Powered Transfemoral Prostheses," *IEEE Robotics and Automation Letters*, vol. 6, no. 3, pp. 5113–5120, 2021.
- [27] A. Naeem *et al.*, "Virtual constraint control of Knee-Ankle prosthesis using an improved estimate of the high phase-variable," *Biomedical Signal Processing and Control*, vol. 73, no. 103366, 2022.
- [28] A. Shumway-Cook, S. Brauer, and M. Woollacott, "Predicting the probability for falls in community-dwelling older adults using the timed up and go test," *Phys. Ther.*, vol. 80, no. 9, pp. 896–903, 2000.
- [29] W. Dite, H. J. Connor, and H. C. Curtis, "Clinical Identification of Multiple Fall Risk Early After Unilateral Transtibial Amputation," *Arch. Phys. Med. Rehabil.*, vol. 88, no. 1, pp. 109–14, 2007.
- [30] T. Elery, S. Rezaazadeh, C. Nesler, and R. D. Gregg, "Design and validation of a powered knee-ankle prosthesis with high-torque, low-impedance actuators," *IEEE Trans. Robot.*, vol. 36, no. 6, pp. 1649–1668, 2020.
- [31] J. Vantilt *et al.*, "Model-based control for exoskeletons with series elastic actuators evaluated on sit-to-stand movements," *J. NeuroEng. Rehabil.*, 2019.
- [32] D. A. Winter, H. G. Sidwall, and D. A. Hobson, "Measurement and reduction of noise in kinematics of locomotion," *Journal of Biomechanics*, vol. 7, no. 2, pp. 157–9, 1974.
- [33] S. L. Whitney, D. M. Wrisley, G. F. Marchetti, M. A. Gee, M. S. Redfern, and J. M. Furman, "Clinical measurement of sit-to-stand performance in people with balance disorders: Validity of data for the Five-Times-Sit-to-Stand Test," *Phys. Ther.*, vol. 85, no. 10, pp. 1034–1045, 2005.